



Published in final edited form as:

*Cancer Res.* 2009 January 1; 69(1): 300–309. doi:10.1158/0008-5472.CAN-08-2145.

## Identification of Novel Alternative Splice Isoforms of Circulating Proteins in a Mouse Model of Human Pancreatic Cancer

Rajasree Menon<sup>1</sup>, Qing Zhang<sup>2</sup>, Yan Zhang<sup>1</sup>, Damian Fermin<sup>1</sup>, Nabeel Bardeesy<sup>3</sup>, Ronald A. DePinho<sup>4</sup>, Chunxia Lu<sup>5</sup>, Samir M. Hanash<sup>2</sup>, Gilbert S. Omenn<sup>1</sup>, and David J. States<sup>1</sup>

<sup>1</sup>Center for Computational Medicine and Biology, University of Michigan, Ann Arbor, MI

<sup>2</sup>Fred Hutchinson Cancer Research Center, Seattle, WA

<sup>3</sup>Center for Cancer Research, Massachusetts General Hospital, Boston, MA

<sup>4</sup>Center for Applied Cancer Science, Dana-Farber Cancer Institute and Harvard Medical School, Boston, MA

<sup>5</sup>Pediatric Endocrinology, University of Michigan, Ann Arbor, MI

### Abstract

To assess the potential of tumor-associated alternatively spliced gene products as a source of biomarkers in biological fluids, we have analyzed a large dataset of mass spectra derived from the plasma proteome of a mouse model of human pancreatic ductal adenocarcinoma. MS/MS spectra were interrogated for novel splice isoforms using a non-redundant database containing an exhaustive 3-frame translation of Ensembl transcripts and gene models from ECgene. This integrated analysis identified 420 distinct splice isoforms, of which 92 did not match any previously annotated mouse protein sequence. We chose seven of those novel variants for validation by reverse transcription polymerase chain reaction (RT-PCR). The results were concordant with the proteomic analysis. All seven novel peptides were successfully amplified in pancreas specimens from both wild-type and mutant mice. Isotopic labeling of cysteine-containing peptides from tumor-bearing mice and wild-type controls enabled relative quantification of the proteins. Differential expression between tumor-bearing and control mice was notable for peptides from novel variants of muscle pyruvate kinase, malate dehydrogenase 1, glyceraldehyde-3-phosphate dehydrogenase, proteoglycan 4, minichromosome maintenance, complex component 9, high mobility group box 2 and hepatocyte growth factor activator. Our results show that, in a mouse model for human pancreatic cancer, novel and differentially expressed alternative splice isoforms are detectable in plasma and may be a source of candidate biomarkers.

### Keywords

Alternative splice variant protein; proteomics; Pancreatic cancer

### Introduction

Alternative splicing plays an important role in protein diversity without significantly increasing genome size. Aberrations in alternative splice variants contribute to a number of diseases including cancers (1,2). For example, Thorsen et al (2) identified cancer-specific splicing events in colon, bladder, and prostate tissues, with diagnostic and prognostic implications. The several alternatively spliced sequence databases now publicly available differ in their annotation and modeling methods and contain many transcripts not present in reference resources like Ensembl or Refseq (3). The ECgene database is one of the largest alternatively

spliced sequence databases (4). Entries in this database are scored as high, medium, or low confidence reflecting the amount of cumulative evidence in support of the existence of a particular alternatively spliced sequence. Evidence is collected from clustering of ESTs, mRNA sequences and gene model predictions. We modified the ECgene database to include three-frame translations of the cDNA sequences (5) to determine the occurrence of novel splice variant proteins. An important development in recent years is substantial improvement in tandem mass spectrometry instrumentation for proteomics, allowing in-depth analysis and confident identifications even for proteins coded by mRNA transcript sequences expressed at low levels (6-8).

Pancreatic ductal adenocarcinoma (PDAC) is among the most lethal of human cancers due to absence of methods for early diagnosis and chemoresistance of advanced disease. The Kras<sup>G12D</sup>/Ink4a/Arf mouse model of PDAC was engineered with signature mutations that recapitulate the histopathologic progression of the human disease in a highly reproducible and synchronous fashion (9,10). Here we exploit this model to test the hypothesis that cancer-specific alternative splice variants can be identified by in-depth mass spectrometric analysis of plasma proteins from this mouse model of pancreatic cancer. In this study, we have interrogated our modified ECgene database to identify both novel and known splice variants among circulating proteins. In addition, our analysis of quantitative expression ratios reveals variant proteins that are differentially expressed in pancreatic cancer.

## Materials and Methods

### Mass spectrometry data

Our search for alternative spliced forms used data from extensive proteomic analysis of plasma from 7 weeks old male wild type mice and KRas<sup>G12D</sup>/Ink4a-Arf mouse model of PDAC (10). Approximately 1/3 of the Kras Ink4a/Arf mice present with the most common pathology observed in human cases – glandular. Plasma from Kras Ink4a/Arf mice with exclusively glandular tumor areas were used in this study. The samples were processed by Intact Protein Fractionation and Analysis System (11) protocol which incorporates immunodepletion to eliminate the most abundant plasma proteins, thus removing 90% of the protein mass. Immunodepletion was followed by isotopic labeling of protein cysteine residues with acrylamide, heavy (D3) for mutant and light (D0) for wild type samples. The mass difference between a D3 labeled and a D0 labeled cysteine residue is 3.01884 daltons. Samples from wild type and PDAC bearing mice were then pooled and the intact proteins were fractionated into 12 anion exchange (AX) fractions followed by 13 or more reverse phase (RP) fractions for each AX fraction yielding a total of 163 fractions. Individual fractions were digested with trypsin and analyzed using a ThermoFinnigan LTQ-FT mass spectrometer. Mass spectra from the LTQ-FT experiment were acquired as RAW files. The mzXML files containing the spectral information were extracted from RAW files using ReAdW.exe program (<http://tools.proteomecenter.org>). The mzXML files were then searched against a modified ECgene database (for alternate splice variant analysis) using X!Tandem (12) software.

### Modified ECgene Database

Alternative splicing can generate multiple transcripts from the same gene which are translated to splice isoforms (also known as splice variant proteins). Our target alternative splice variant protein database, the modified ECgene database, was constructed by combining Ensembl 40 and ECgene database (mm8, build 1). Taking alternative splicing events into specific consideration, ECgene combines genome-based EST clustering and the transcript assembly procedure to construct gene models that encompass all alternative splicing events. The reliability of each isoform is assessed from the nature of cluster members and from the minimum number of clones required to reconstruct all exons in the transcript (13). The ECgene

database contains a total of 417,643 splice variants. In the Ensembl 40 database, there is a total of 21,839 mouse genes with 28,110 transcripts, of which 10,922 alternative transcripts are derived from 4,651 genes.

Transcript sequences from the ECgene and Ensembl 40 databases were translated in three reading frames. Within each dataset, the first instance of each protein sequence longer than 14 amino acids was recorded. The resulting proteins from both database translations were then combined and filtered for redundancy. For this filtering, proteins derived from Ensembl transcripts were preferentially recorded over those generated from ECgene records. A collection of common protein contaminant sequences was added to this set. Lastly, all sequences were reversed and appended to the set of forward sequences as an internal control for false identifications. This last step resulted in doubling the total number of entries in the modified ECgene database with a final total of 10,381,156 protein sequences.

### Post search analyses

**Trans Proteomic Pipeline (TPP)**—For statistical purposes, the X!Tandem search results were post processed with PeptideProphet and ProteinProphet software using TPP (version 3.2) (<http://tools.proteomecenter.org>). First, we analyzed search results from each fraction separately using PeptideProphet, and then processed all PeptideProphet files together using ProteinProphet. Relative quantification of isotopically labeled peptides was performed using the Q3Ratio (14) and XPRESS (15) applications in TPP. The relative abundance of a peptide can be calculated, by reconstructing the light and heavy elution profiles of the precursor ions and by determining the elution areas of each peak. From Q3Ratio and XPRESS analyses, we obtained the average expression ratio (mutant/wildtype) for those peptides that were unique to the splice variant protein identified and had labeled cysteine residue.

**Michigan Peptide to Protein Integration (MPPI)**—In addition to the TPP analysis, we implemented a second analysis based on selecting all peptide identifications with X!Tandem expect score of  $\leq 0.001$ . We applied an integration process to these peptide identifications which greatly reduced the set of proteins and retained all of the peptide identifications. The integration process was as follows:

1. A list of all peptide matches was created.
2. The peptide list was ordered by the number of spectra matching each peptide.
3. Peptide with largest number of matching spectra was selected.
4. A list of all proteins containing this peptide was made.
5. The protein list was sorted by the number of spectra matching peptides derived from the protein.
6. The protein with the largest number of matching spectra and which was identified by largest number of distinct peptides was selected. When equal numbers of identifying spectra were present, Ensembl proteins were given preference because these transcripts have been independently reviewed and Ensembl identifiers can readily be linked to additional annotation.
7. All peptides contained within this protein were removed from the peptide list.
8. Steps 3-7 were repeated until no peptides remained in the peptide list.

Protein identifications based on a single peptide from this MPPI analysis were retained only if identified by at least ten distinct spectra. For further analyses we used the union of protein identifications from TPP analysis with ProteinProphet probability  $> 0.9$  and the MPPI. To

remove redundant protein identifications, we ran another round of MPPI using all peptides found in either TPP or first phase MPPI (Figure 1).

### Sequence analysis for novel proteins

The peptide sequences for which the alternative splice variant proteins were identified, were searched against the mouse genome (Build 37) using UCSC BLAT (16) browser and against NR using NCBI blastp (17). In some cases, when the peptide sequences are short, the blat or blastp programs were not able to align correctly. To handle these cases and verify search results, we further searched the peptide sequences against nr protein sequences by SQL pattern match. Proteins whose peptide sequences aligned perfectly to an existing canonical mouse coding sequence were removed from the list of alternatively spliced protein identifications. The identifications that remain after this round of blat and blastp analysis must be novel as all their peptides did not precisely match to any known mouse proteins. We subsequently checked whether any peptides of these novel identifications matched either partially or completely to any known protein sequences using blastp. If a match is observed, those identifications were considered as novel splice variants of known genes.

### Validation of the novel peptides by RT-PCRs

In order to corroborate the identifications of novel splice variants, peptide sequences with splice variations from seven novel variants were selected for validation by reverse transcription polymerase chain reaction (RT-PCR) (Figure 4). We chose these seven peptide sequences as they were identified by multiple high scoring spectra (X!Tandem expect value < 0.001) (Supplementary Table 8) and are much less annotated than splice variants of apolipoproteins, complement component proteins, hemopexin and vitamin D binding protein, which were also identified. The primers were designed using the Primer3 software (<http://frodo.wi.mit.edu>) from the cDNA sequences of these 7 proteins in the ECGene database (Supplementary Table 8). Total RNA was extracted from frozen pancreatic tissue of wild type and mutant mice using TRIzol reagent (Invitrogen, CA, USA) in accordance with the manufacturer's instructions. RNA purification was performed using the RNeasy Mini Kit (Qiagen Inc., Valencia, CA) and Rnase-Free Dnase digestion (Qiagen Inc., Valencia, CA). Qiagen one Step RNA PCR Kit (AMV) was used for RT-PCR amplification of the seven novel peptides from total RNA. Primers for amplifying gamma actin (Forward: 5'- GCGCAAGTACTCTGTGTGGA -3'; Reverse: 5'- ACATCTGCTGGAAGGTGGAC-3') were used to amplify the house keeping gene as a positive control and standard for quantification.

After incubation at 50 °C for 30 min, 1 cycle of 94 °C for 15 min and 40 cycles of 94 °C 30 sec, 50 °C 30 sec, 72 °C 1 min followed by 72 °C 10 min for final extension were performed using the thermal cycler MJ PTC 200 (BioRad, USA). Amplicons were run on 2% agarose gel and visualized under UV light. Images were captured using a gel imaging system (biostep GmbH, Germany).

**Quantitative RT-PCR**—Four of these seven novel peptides chosen above for RT-PCR showed differential expression by TPP expression ratio analyses. These peptides include pyruvate kinase variant, malate dehydrogenase 1 variant, PCTAIRE-motif protein kinase 2 variant and solute carrier family 19 (sodium/hydrogen) variant. The mRNA expression levels of these four novel peptides were measured by quantitative real-time PCR using a QuantiTect SYBER Green PCR (Qiagen) and ABI Prism 7000 Sequence Detector (Applied Biosystems). The expression of gamma actin was determined as an internal control. The PCR amplification reaction and the detection of PCR product was monitored by measuring the increase in fluorescence intensity caused by the binding of SYBER Green dye to double-stranded (ds) DNA. The same RT-PCR primers (Supplementary Table 8) were used in this method. PCR amplification was performed using the following profile: 1 cycle at 50°C for 30min, 1 cycle

at 95°C for 10min, and 40 cycles at 94°C for 15s, 60°C for 1min. Calculations for relative quantification were performed as outlined in User Bulletin #2: ABI Prism 7700 Sequence Detection System (PE Applied Biosystems) (18).

Since we had access to only a single sample of pancreatic tissue from the wild type and mutant mice, respectively, we are unable to do biological sample replicates. However, we performed the quantitative RT-PCR three times using the same two samples to assess technical errors.

### Functional annotation

The gene ontology (GO) annotation file for *Mus musculus*, was downloaded from <http://www.geneontology.org/GO.current.annotations.shtml> site and the GO terms associated with the parent gene symbols of the splice variants were studied. The functional annotations of the splice isoforms were done by searching the parent gene names using FuncAssociate (19). FuncAssociate is a web-based tool that accepts as input a list of genes, and returns a list of GO attributes that are over- (or under-) represented among the genes in the input list. Only those over- (or under-) representations that are statistically significant, after correcting for multiple hypotheses testing, are reported.

## Results

### Summary of protein identifications

The mass spectra derived from plasma protein analysis were searched against the modified ECgene database using X!Tandem. The empirical false discovery rate (FDR) calculated based on peptide identifications from reverse protein sequences was < 0.5% for all peptide identification scoring bins with X!tandem expect score < 0.001 (Supplementary Figure 1). Protein and peptide identifications from the X!Tandem search and post-search TPP/MPPI analysis are summarized in Table 1. Figure 1 summarizes the analysis workflow. TPP analysis of the search results yielded 1150 proteins with ProteinProphet probability  $\geq 0.9$  (FDR for proteins < 1.5%). In parallel, using our MPPI method (expect < 0.001), we identified a total of 1063 proteins (FDR for proteins < 1.5%). There were 870 biological proteins identifications and 3 reverse sequences found in common by both approaches. Thus, the empirical FDR for proteins identified by both methods is < 0.3%. The union of the TPP and MPPI methods resulted in 1340 protein identifications. There were 467 biological proteins and 22 reverse sequences identified by either TPP or MPPI but not by both. Thus, the empirical FDR for proteins identified by either but not both methods is < 5%. The reverse sequence proteins identified by TPP and MPPI analyses were different; since we took the union of protein identifications from both methods, the false discovery rate at the protein identification level increased.

Taking the union of the two methods introduces some redundancy in identifications so we applied a second round of MPPI on these 1340 proteins yielding 1278 distinct protein identifications with 25 proteins from reverse sequence. Of the 1278 protein identifications, 420 were splice variant proteins (Supplementary Table 1).

### Novel alternative splice variant protein identifications

To identify novel spliced sequences, we searched the peptide sequences of the 420 alternative splice proteins against the Mouse genome using blat and against NR database using blastp (see Methods); 92 of 420 alternative splice proteins were identified by unique peptides that did not align completely with any known mouse coding sequence (Figure 1, Supplementary Table 2). These proteins are considered novel identifications. Of these 92 identifications, 84 were novel alternative splice variants of known genes. An example is the identification of novel variant for peptidase inhibitor 16 (*pil6*) by the unique peptide 'ATEAPSSRETGAENPEK'. Figure 2 shows the alignment of this peptide to the known *pil6* sequence by blastp. The alignment

suggests a partial deletion (230 amino acids) of the exon sequence due to a splicing event resulting in the novel variant.

For 8 identifications from the 92 novel proteins, neither the complete protein sequence nor the peptides identified matched even partially to any known mouse proteins by blastp. (parent gene name and gene symbol is given as null in Supplementary Table 2). However, we found that the complete protein sequences of these 8 proteins matched perfectly to various mouse genomic regions (Supplementary Table 3).

Both known and novel variant forms of many genes were found in the 420 protein set. For example, we found seven variants of alpha-2-HS-glycoprotein including three known and four novel variant forms. A particularly interesting example is the identification of known and novel isoforms of muscle pyruvate kinase; the novel alternative splice variant, 'M9C5102\_13\_s4154\_e5807\_1\_rf0\_c1\_n0|', was identified by the unique peptide 'CLAAALIVLTESGR' from five different spectra. This peptide sequence did not align to the coding sequence of annotated mouse muscle pyruvate kinase protein. However, it aligned to human, rat and chicken muscle pyruvate kinase M1 isoform (Figure 3a). The previously known mouse gene product for muscle pyruvate kinase (*pkm2*) gene, which is homologous to the M2 isoform of human and rat *pkm2*, was identified by 25 distinct peptides, 22 of which were shared by the novel mouse variant protein. Figure 3b shows identifications of unique peptides of a known isoform mouse malate dehydrogenase protein and its novel splice form from different clusters of reverse phase fractions; the isoform exhibits faster mobility by reversed phase chromatography.

### Tumor related novel alternative splice variant proteins

By combining the Q3Ratio and XPRESS analyses, we calculated expression ratios for the cysteine containing unique peptides with splice variation from tumor bearing mice relative to controls for 28 of 92 novel splice variant proteins (Table 2). The unique peptides from sixteen variants were identified by multiple spectra, which enabled us to calculate the 95% confidence intervals for their expression ratios. Splice variants of malate dehydrogenase 1, muscle pyruvate kinase, proteoglycan 4, complement component factor H, major urinary protein, vitamin d binding protein and alpha-2-HS-glycoprotein had the 95% confidence intervals for their expression ratios greater than 1 (Table 2). However, expression ratios of unique peptides of twelve variants were calculated from single spectrum. Six of these proteins showed greater than two-fold expression ratios; splice variants of high mobility group box 2 protein and minichromosome maintenance complex component 9 are in this group. The other six proteins include novel variants of alpha fetoprotein, peroxiredoxin 2 and solute carrier family 19 member1.

Alpha fetoprotein, Apolipoprotein e, Ceruloplasmin, Fibronectin, Glyceraldehyde 3 phosphate dehydrogenase, Hemopexin, Peptidylprolyl isomerase, and Tubulin alpha are among proteins previously identified as involved in pancreatic cancer (20-22). It is noteworthy that in our 92 novel proteins, we identified the presence of additional novel alternative splice variants of these proteins.

### RT-PCR validations

The identifications of novel alternative splice variants were further validated by checking the mRNA expressions of seven peptide sequences with splice variations (Supplementary Table 8) by RT-PCR. The results were concordant with our proteomic analysis. All seven novel peptide coding sequences were amplified in both wild type and mutant samples (Figure 4a). Amplified sequences ranged in size from 63 -75 bp (Figure 4a). In addition, we did the QT-PCR on four peptides which showed differential expression by TPP analysis (Figure 4b). The

expression profile for novel variants of *pkm2* and *pctk2* were similar to what we observed by TPP analysis. However, the expression profiles of novel variant of *mdh1* and *soll19a1* were opposite to what we observed from TPP analysis. We saw decreased mRNA expression of the novel *mdh1* peptide in mutant sample versus the wild type. Even though the unique peptide for *soll19a1* variant was identified by multiple spectra, the expression ratio was calculated by Q3Parser from a single spectrum.

### Functional annotations of novel alternative splice variant proteins

Gene Ontology (GO) terms associated with the parent gene symbols of the novel splice variants of known proteins are given in Supplementary Table 4. As expected, many proteins were extracellular. However, we observed splice variants of such nuclear proteins as high-mobility group box 2, DEAD box polypeptide 6, nuclear factor interleukin 3 regulated, and peptidylprolyl isomerase like 2. In the molecular function category, more splice variants were associated with metal ion binding and endopeptidase inhibitor activity. Under biological processes, many variants were involved in transport. Supplementary Table 5 summarizes the list of genes with over-represented GO attributes using FuncAssociate.

### Known alternative splice variant proteins

As mentioned earlier, 420 of the 1278 protein identifications were alternative splice variant proteins. By sequence analysis of the peptides identified from these 420 proteins, 92 were found as novel splice proteins. The peptides from the remaining 328 protein identifications matched to sequences from known mouse coding sequences. Variant proteins of many genes previously reported as involved in pancreatic cancer are in this list (Supplementary Table 6a). In addition, variants of genes that were reported by other studies to be involved in other types of cancers are found in this set (Supplementary Table 6b).

Relative expression analysis by Xpress and Q3Proteinparser produced expression ratios for 81 proteins out of 328 known splice variants (Supplementary Table 7). 48 of them had greater than two fold expression at 95% or more confidence interval in mutant samples relative to wild type. According to the analysis, the unique peptide that identified secreted and transmembrane 1A (*sectm1a*) showed the highest fold change in mutant samples. This protein was reported to have potential importance in hematopoietic and/or immune system processes (23).

Ten possible pancreatic cancer biomarkers were chosen by a parallel study on the same mouse model plasma samples (24). Variants of three of these genes are found in our list of 420 splice variant proteins: lipocalin2 (*lcn2*), regenerating islet-derived 3 (*reg3a*) and TNF receptor superfamily, member 1A (*tnfrsf1a*). According to our expression analysis, *tnfrsf1a* showed > 2-fold change in expression in tumor samples compared to wild type.

## Discussion

Alternative splicing allows a single gene to generate multiple mRNAs, which can be translated into functionally and structurally diverse proteins (25). One gene can have multiple variants coexisting at different concentrations, so estimating the relative abundance of each variant may be important for the study of its biological role (25). As reported here, 1278 distinct proteins (Figure 1) were identified from the union of TPP and MPPI analyses; 92 proteins were novel proteins. Successful RT-PCR amplifications of all seven selected novel peptide coding sequences from both wild type and mutant samples validated our protein identifications (Figure 4).

In 28 of the 92 novel variants identified, expression ratios were quantified for mutant and wild-type plasma samples (Table 2). The main reasons why expression ratios could not be quantified

in other cases are the small proportion of cysteine-containing peptides (site of labeling) in the 92 splice variants identified; 774 of 2513 peptides from 92 splice variants contain cysteine residues. Further, the XPRESS and Q3Ratio quantification software reported only 'heavy' or 'light' expression for many peptides; to quantify the relative expression ratio, both values are needed. The quantifications of mRNA expression by QT-PCR were concordant with protein expression for two of the four peptides verified. The inverse correlation observed mRNA-protein expression in the other two peptides might be due to numerous factors, including negative feedback by the protein variant on mRNA synthesis, post-transcriptional control of protein translation, and protein modifications. There are several studies showing varying correlation between mRNA and protein abundance ratios (26,27). Guo et al (28), in their correlation analyses on mRNA-protein expression in freshly isolated human circulating monocytes, found some genes with moderate and varied correlations, suggesting that mRNA expression might be sometimes useful, but is not reliable in predicting protein expression levels.

Many of the known protein variants that we identified have been reported as involved in pancreatic or other types of cancer, some with significant differential expression, such as acyl co-A acetyltransferase, chromogranin b, granulin, insulin like growth factor binding protein 2 and regenerating islet-derived 3 alpha (Supplementary Table 6 for citations, Supplementary Table 7 for expression ratios).

The focus of our work is on the novel variants, of which we annotate eight. First, we highlight three novel splice proteins with > 2-fold increase in mutant plasma compared to wild type which may have potential role in progression of pancreatic cancer: pyruvate kinase (*pkm2*), proteoglycan 4 (*prg4*) and malate dehydrogenase 1 (*mdh1*). The 95% confidence intervals for their > 2-fold expression ratios exclude unity.

Pyruvate kinase, a glycolytic enzyme, catalyzes transfer of a phosphoryl group from phosphoenolpyruvate (PEP) to ADP, generating ATP. Most adult tissues express the M1 isoform of pyruvate kinase whereas embryonic tissues and tumors express the M2 isoform. Christofk et al (29,30) demonstrated that the M2 isoform of muscle pyruvate kinase accounts for the long known distinctive Warburg effect of shift to aerobic glycolysis in tumor cells. The novel mouse peptide sequence 'CLAAALIVLTESGR' with which we identified the novel splice variant of muscle pyruvate kinase was from five different spectra, authenticating the occurrence of this variant. In addition, our study shows that the mRNA and peptide expressions of this novel variant were positively correlated for this gene and show increased expression in mutant samples compared to wild type. The peptide sequence is identical to the human, rat and chicken pyruvate kinase M1 variant (Figure 3a). A second variant of pyruvate kinase, M2 type pyruvate kinase, was also identified in our 420 alternative splice isoform list. All the 25 peptides identified in this protein aligned completely with known mouse coding sequence. Studies by Kumar et al (31) and Ventrucci et al (32) report tumor type *pkm2* as a metabolic marker specifically for pancreatic cancer.

*Prg4* has been identified as megakaryocyte stimulating factor and articular superficial zone protein. *Prg4* has characteristic motifs including somatomedin B and hemopexin domains, a chondroitin sulfate-attachment site and mucin-like repeats (33). The specific role of *prg4* in the articular joint has previously been reported; however, the presence of multi-functional motifs and the identification of a novel variant suggest that *prg4* functions in several distinctive biological processes. Faca et al (24) observed an increased gene expression of isoform E of *prg4* in human pancreatic cancer samples.

*Mdh1* is an enzyme in the citric acid cycle that catalyzes the conversion of malate into oxaloacetate and vice versa. It also plays a role in gluconeogenesis. Impaired oxidative

metabolism may contribute to malignant growth (34). *Mdh1* has been reported as over-expressed in thyroid oncocytic tumors (35). Over-expression of the novel variant of *mdh1* in our study suggests that cellular energy pathways may play an important functional role in tumor progression.

The novel peptide 'CELAEQMTSLLER' was identified by eight different spectra. Both mRNA and protein expression of this peptide were down regulated in mutant samples when compared to that of wild type. Blasting this peptide sequence against NCBI-nr database showed that part of the peptide 'ELAEQMT' aligned perfectly with mouse PCTAIRE-motif protein kinase 2 (*pctk2*). Valladares et al (36) showed over-expression of *pctk2* in breast cancer samples from Mexican women. The PCTAIRE protein kinases comprise a distinct subfamily of the cell division controller 2 (*cdc2*) related serine/threonine-specific protein kinases. Deregulation of cell-cycle control is thought to be a crucial event in malignant transformation. Guo et al (37) demonstrate an important role of *cdc25b* in cell-cycle progression, raising the possibility that inhibition of *cdc25b* may have therapeutic potential in pancreatic cancer.

Another novel variant with increased expression in our peptide expression analysis is minichromosome maintenance complex component 9 variant. MCM proteins are well-known regulators of the cell cycle. *Mcm9* binds to chromatin in an ORC-dependent manner and is required for the recruitment of the *Mcm2-7* helicase onto chromatin (38). Further, MCM family members 2 and 5 are markers of aggressive cervical and other cancers (39). *Mcm9* and *mdh1* have not been reported as involved in pancreatic cancer. It would be interesting to investigate potential roles of these novel variants in pancreatic cancers.

A splice variant of high mobility group box 2 (*hmgb2*) showed > 2-fold increase in expression in mutant samples. *Hmgb2* is involved in DNA repair. It has not been reported as upregulated in pancreatic cancer, but this gene is located at 4q32-34, a region identified as a potential locus for familial pancreatic cancer in a large American family (40).

Another interesting protein is the novel splice variant of hepatocyte growth factor activator (*hgfa*), a serine protease that converts the inactive single-chain precursor of hepatocyte growth factor (*hgf*) to the active heterodimer in response to tissue injury (41). Results from Lee et al (42) suggest that extracellular receptor kinase activation by *hgf* might be important in pancreatic cancer metastasis.

We found many novel splice variants to glyceraldehyde-3-phosphate dehydrogenase (*gapdh*), another critical enzyme in glycolysis. *Gapdh* mRNA levels are over-expressed in many cancers; relative levels correlate with pathologic stage in prostate cancer (43-45). Chen et al (21) observed > 2-fold increase of *gapdh* in pancreatic cancer tissue using isotope-coded affinity tag (ICAT) technology followed by mass spectrometry.

The ECgene (<http://genome.ewha.ac.kr/ECgene/>) database uses the ECgene gene prediction algorithm to identify splice variants by EST clustering. Three levels of confidence (high, medium and low) were set on the gene models based on mRNA evidence (13). The custom built ECgene database used for our study has another layer of complexity which is the 3-frame translation of ECgene sequences of predicted gene models, which makes it feasible to identify novel proteins. We found 8 proteins where no peptides matched to any known mouse protein sequences by blastp analysis (Supplementary Table 3); Three proteins (M14C7677\_1\_s356\_e431\_1\_rf1\_c1\_n0|, M5C5274\_1\_s2\_e95\_1\_rf0\_c1\_n0|, and M1C10834\_9\_s770\_e824\_1\_rf2\_c1\_n0|) had differential expression in mutant samples relative to wild type. Further investigation of these novel proteins in pancreatic cancer appears warranted.

One focus in cancer biomarker discovery is driven by the approach that the most promising plasma biomarkers will be secreted proteins (46). Gene Ontology analysis of the novel splice variants by FuncAssociate showed extracellular as a top-ranking attribute (Supplementary Table 5). Interestingly, the unique peptide with which we identified the novel protein M5C6460\_1\_s86\_e1988\_1\_rf0\_c1\_n0 had a 71% sequence similarity to the peptide sequence of the extracellular protein, alpha fetoprotein, a 'gold-standard' in the field of tumor markers (47). According to FuncAssociate analysis, endopeptidase inhibitor/endoproteinase inhibitor/proteinase inhibitor activity (GO: 0004866) is a top-ranking Gene Ontology attribute. Imbalanced protease activity has long been recognized in progression of cancers and inflammation (48). Other high-ranking biological processes are glucose metabolism and lipid transport. There are many studies linking impaired glucose metabolism and pancreatic cancer (49,50). Supplementary Table 4 shows aldolase c, *gapdh*, *mdh1* and *pkm2* as genes involved in glucose metabolism. The differential expression for novel alternative splice variants of *gapdh*, and *mdh1* suggest involvement of these splice variants in tumors.

The combined proteomic and bioinformatic approach in this study has identified many novel splice variant proteins, including many with differential expression in plasma from mutant mice with *Kras*<sup>G12D</sup>/*Ink4a*/*Arf* mediated pancreatic cancer versus wild type mice. These differentially-expressed splice variant proteins may influence many cancer-related mechanisms. The data suggest that alternative splice variant proteins are a potentially rich source of candidate biomarkers for cancers.

## Supplementary Material

Refer to Web version on PubMed Central for supplementary material.

## Acknowledgements

The authors thank Dr. Thomas Blackwell for giving helpful suggestions in statistical analysis.

Funding: This work was supported in part by NCI/SAIC contract N01-CO-12400/Sub-k 323XS110A on Mouse Models of Human Cancers, MTTC GR 687 for Proteomics Alliance for Cancer Research, R01 LM008106 Automated Genome Annotation, MMHCC U01 CA84313, NCI PDAC P01 IPOICA117969-01, U54 DA021519 National Center for Integrative Biomedical Informatics, P41 RR018627 National Resource for Pathways and Proteomics, and U01 CA 084982 NCI Early Detection Research Network.

## References

1. Klinck R, Bramard A, Inkel L, et al. Multiple alternative splicing markers for ovarian cancer. *Cancer Res* 2008;68(3):657–63. [PubMed: 18245464]
2. Thorsen K, Sorensen KD, Brems-Eskildsen AS, et al. Alternative splicing in colon, bladder, and prostate cancer identified by exon-array analysis. *Mol Cell Proteomics* 2008;7(7):1214–24. [PubMed: 18353764]
3. Larsson TP, Murray CG, Hill T, Fredriksson R, Schiöth HB. Comparison of the current RefSeq, Ensembl and EST databases for counting genes and gene discovery. *FEBS Letters* 2005;579(3):690–8. [PubMed: 15670830]
4. Kim P, Kim N, Lee Y, Kim B, Shin Y, Lee S. ECGene: genome annotation for alternative splicing. *Nucl Acids Res* 2005;33(suppl1):D75–9. [PubMed: 15608289]
5. Fermin D, Allen B, Blackwell T, et al. Novel gene and gene model detection using a whole genome open reading frame analysis in proteomics. *Genome Biology* 2006;7(4):R35. [PubMed: 16646984]
6. Wang R, Prince JT, Marcotte EM. Mass spectrometry of the *M. smegmatis* proteome: Protein expression levels correlate with function, operons, and codon bias. *Genome Res* 2005;15(8):1118–26. [PubMed: 16077011]
7. Ideker T, Thorsson V, Ranish JA, et al. Integrated Genomic and Proteomic Analyses of a Systematically Perturbed Metabolic Network. *Science* 2001;292(5518):929–34. [PubMed: 11340206]

8. Hanash SM, Pitteri SJ, Faca VM. Mining the plasma proteome for cancer biomarkers. *Nature* 2008;452(7187):571–9. [PubMed: 18385731]
9. Bardeesy N, Aguirre AJ, Chu GC, et al. From the Cover: Both p16Ink4a and the p19Arf-p53 pathway constrain progression of pancreatic adenocarcinoma in the mouse. *Proceedings of the National Academy of Sciences* 2006;103(15):5947–52.
10. Aguirre AJ, Bardeesy N, Sinha M, et al. Activated Kras and Ink4a/Arf deficiency cooperate to produce metastatic pancreatic ductal adenocarcinoma in the mouse. *Genes Dev* 2003;17(24):3112–26. [PubMed: 14681207]
11. Wang H, Clouthier SG, Galchev V, et al. Intact-protein-based High-resolution Three-dimensional Quantitative Analysis System for Proteome Profiling of Biological Fluids. *Mol Cell Proteomics* 2005;4(5):618–25. [PubMed: 15703445]
12. Craig R, Beavis RC. TANDEM: matching proteins with tandem mass spectra. *Bioinformatics* 2004;20(9):1466–7. [PubMed: 14976030]
13. Kim N, Shin S, Lee S. ECGene: Genome-based EST clustering and gene modeling for alternative splicing. *Genome Res* 2005;15(4):566–76. [PubMed: 15805497]
14. Faca V, Coram M, Phanstiel D, et al. Quantitative Analysis of Acrylamide Labeled Serum Proteins by LC-MS/MS. *J Proteome Res* 2006;5(8):2009–18. [PubMed: 16889424]
15. Han DK, Eng J, Zhou H, Aebersold R. Quantitative profiling of differentiation-induced microsomal proteins using isotope-coded affinity tags and mass spectrometry. *Nat Biotech* 2001;19(10):946–51.
16. Kent WJ. BLAT---The BLAST-Like Alignment Tool. *Genome Res* 2002;12(4):656–64. [PubMed: 11932250]
17. McGinnis S, Madden TL. BLAST: at the core of a powerful and diverse set of sequence analysis tools. *Nucl Acids Res* 2004;32(suppl2):W20–5. [PubMed: 15215342]
18. Livak K. ABI Prism 7700 Sequence Detection System. User Bulletin 2 PE Applied Biosystems. 1997
19. Berriz GF, King OD, Bryant B, Sander C, Roth FP. Characterizing gene sets with FuncAssociate. *Bioinformatics* 2003;19(18):2502–4. [PubMed: 14668247]
20. Gronborg M, Kristiansen TZ, Iwahori A, et al. Biomarker Discovery from Pancreatic Cancer Secretome Using a Differential Proteomic Approach. *Mol Cell Proteomics* 2006;5(1):157–71. [PubMed: 16215274]
21. Chen R, Brentnall TA, Pan S, et al. Quantitative Proteomics Analysis Reveals That Proteins Differentially Expressed in Chronic Pancreatitis Are Also Frequently Involved in Pancreatic Cancer. *Mol Cell Proteomics* 2007;6(8):1331–42. [PubMed: 17496331]
22. Matsueda K, Yamamoto H, Yoshida Y, Notohara K. Hepatoid carcinoma of the pancreas producing protein induced by vitamin K absence or antagonist II (PIVKA-II) and  $\alpha$ -fetoprotein (AFP). *Journal of Gastroenterology* 2006;41(10):1011–9. [PubMed: 17096071]
23. Slentz-Kesler KA, Hale LP, Kaufman RE. Identification and Characterization of K12 (SECTM1), a Novel Human Gene That Encodes a Golgi-Associated Protein with Transmembrane and Secreted Isoforms. *Genomics* 1998;47(3):327–40. [PubMed: 9480746]
24. Faca VM, Song KS, Wang H, et al. A Mouse to Human Search for Plasma Proteome Changes Associated with Pancreatic Tumor Development. *PLoS Medicine* 2008;5(6):e123. [PubMed: 18547137]
25. Wang H, Hubbell E, Hu J-s, et al. Gene structure-based splice variant deconvolution using a microarray platform. *Bioinformatics* 2003;19(suppl1):i315–22. [PubMed: 12855476]
26. Gygi SP, Rochon Y, Franza BR, Aebersold R. Correlation between Protein and mRNA Abundance in Yeast. *Mol Cell Biol* 1999;19(3):1720–30. [PubMed: 10022859]
27. Washburn MP, Koller A, Oshiro G, et al. Protein pathway and complex clustering of correlated mRNA and protein expression analyses in *Saccharomyces cerevisiae*. *Proceedings of the National Academy of Sciences of the United States of America* 2003;100(6):3107–12. [PubMed: 12626741]
28. Guo Y, Peng X, Lei S. How is mRNA expression predictive for protein expression? A correlation study on human circulating monocytes. *Acta Biochimica et Biophysica Sinica* 2008;40(5):426–36. [PubMed: 18465028]
29. Christofk HR, Vander Heiden MG, Harris MH, et al. The M2 splice isoform of pyruvate kinase is important for cancer metabolism and tumour growth. *Nature* 2008;452(7184):230–3. [PubMed: 18337823]

30. Christofk HR, Vander Heiden MG, Wu N, Asara JM, Cantley LC. Pyruvate kinase M2 is a phosphotyrosine-binding protein. *Nature* 2008;452(7184):181–6. [PubMed: 18337815]
31. Kumar Y, Gurusamy K, Pamecha V, Davidson B. Tumor m2-pyruvate kinase as tumor marker in exocrine pancreatic cancer a meta-analysis. *Pancreas* 2007;35(2):114–9. [PubMed: 17632316]
32. Ventrucci M, Cipolla A, Racchini C, Casadei R, Simoni P, Gullo L. Tumor M2-Pyruvate Kinase, a New Metabolic Marker for Pancreatic Cancer. *Digestive Diseases and Sciences* 2004;49(7):1149–55. [PubMed: 15387337]
33. Ikegawa S, Sano M, Koshizuka Y, Nakamura Y. Isolation, characterization and mapping of the mouse and human PRG4 (proteoglycan 4) genes. *Cytogenetic and Genome Research* 2000;90(34):291–7.
34. Ristow. Oxidative metabolism in cancer growth. *Current opinion in clinical nutrition and metabolic care* 2006;9(4):339–45. [PubMed: 16778561]
35. Baris O, Savagner F, Nasser V, et al. Transcriptional Profiling Reveals Coordinated Up-Regulation of Oxidative Metabolism Genes in Thyroid Oncocytic Tumors. *J Clin Endocrinol Metab* 2004;89(2):994–1005. [PubMed: 14764826]
36. Valladares A, Hernández NG, Gómez FS, et al. Genetic expression profiles and chromosomal alterations in sporadic breast cancer in Mexican women. *Cancer Genetics and Cytogenetics* 2006;170(2):147–51. [PubMed: 17011986]
37. Guo J, Kleeff J, Li J, et al. Expression and functional significance of CDC25B in human pancreatic ductal adenocarcinoma. *Oncogene* 23(1):71–81. [PubMed: 14712212]
38. Lutzmann M, Méchali M. MCM9 Binds Cdt1 and Is Required for the Assembly of Prereplication Complexes. *Molecular Cell* 2008;31(2):190–200. [PubMed: 18657502]
39. Gonzalez MA, Tachibana KE, Laskey RA, Coleman N. Control of DNA replication and its potential clinical exploitation. *Nat Rev Cancer* 2005;5(2):135–41. [PubMed: 15660109]
40. Earl J, Yan L, Vitone LJ, et al. Evaluation of the 4q32-34 Locus in European Familial Pancreatic Cancer. *Cancer Epidemiol Biomarkers Prev* 2006;15(10):1948–55. [PubMed: 17035404]
41. Miyazawa K, Shimomura T, Kitamura N. Activation of Hepatocyte Growth Factor in the Injured Tissues Is Mediated by Hepatocyte Growth Factor Activator. *J Biol Chem* 1996;271(7):3615–8. [PubMed: 8631970]
42. Lee K, Hyun M, Kim J-R. Growth factor-dependent activation of the MAPK pathway in human pancreatic cancer: MEK/ERK and p38 MAP kinase interaction in uPA synthesis. *Clinical & Experimental Metastasis* 2003;20(6):499–505. [PubMed: 14598883]
43. Tokunaga K, Nakamura Y, Sakata K, et al. Enhanced Expression of a Glyceraldehyde-3-phosphate Dehydrogenase Gene in Human Lung Cancers. *Cancer Res* 1987;47(21):5616–9. [PubMed: 3664468]
44. Schek N, Hall BL, Finn OJ. Increased Glyceraldehyde-3-phosphate Dehydrogenase Gene Expression in Human Pancreatic Adenocarcinoma. *Cancer Res* 1988;48(22):6354–9. [PubMed: 3180054]
45. Rondinelli R, Epner D, Tricoli J. Increased glyceraldehyde-3-phosphate dehydrogenase gene expression in late pathological stage human prostate cancer. *Prostate Cancer* 1997;1(2):66–72.
46. Diamandis EP, van der Merwe D-E. Plasma Protein Profiling by Mass Spectrometry for Cancer Diagnosis: Opportunities and Limitations. *Clin Cancer Res* 2005;11(3):963–5. [PubMed: 15709159]
47. Mizejewski GJ. Biological role of  $\alpha$ -fetoprotein in cancer: prospects for anticancer therapy. *Expert Review of Anticancer Therapy* 2002;2(6):709–35. [PubMed: 12503217]
48. Badola S, Spurling H, Robison K, et al. Correlation of serpin-protease expression by comparative analysis of real-time PCR profiling data. *Genomics* 2006;88(2):173–84. [PubMed: 16713170]
49. Gapstur SM, Gann PH, Lowe W, Liu K, Colangelo L, Dyer A. Abnormal Glucose Metabolism and Pancreatic Cancer Mortality. *JAMA* 2000;283(19):2552–8. [PubMed: 10815119]
50. Permert J, Ihse I, Jorfeldt L, Von Schneck H, Arnqvist H, Larsson J. Pancreatic cancer is associated with impaired glucose metabolism. *European Journal of Surgery* 1993;159(2):101–7. [PubMed: 8098623]

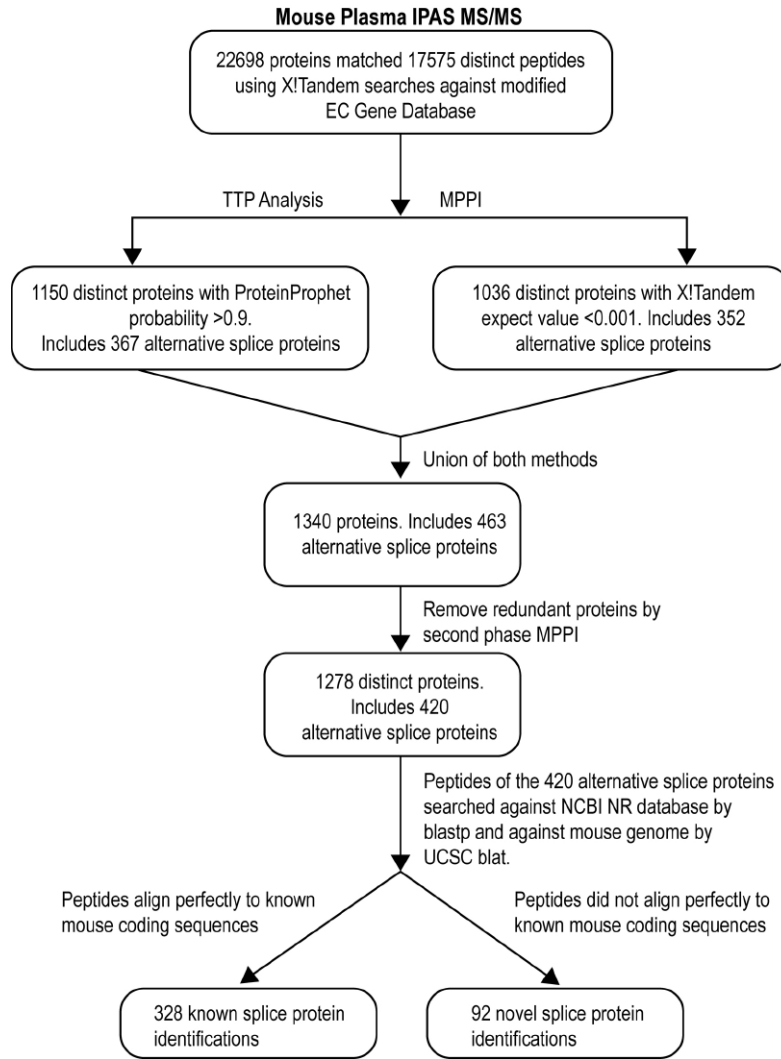


**Figure 1.** Flow chart of multi-step analysis of X!Tandem search results from Intact Protein Analysis System (IPAS) MS/MS combining Trans Proteomic Pipeline (TPP) and Michigan Peptide-to-Protein Integration (MPPI), leading to 92 novel alternative splice variants.

**A**

```

>gb|EDL22615.1| Gene info peptidase inhibitor 16 [Mus musculus]
Length=415
GENE ID: 74116 Pi16 | peptidase inhibitor 16 [Mus musculus]
(10 or fewer PubMed links)
Score = 35.4 bits (76), Expect = 0.52
Identities = 11/11 (100%), Positives = 11/11 (100%), Gaps = 0/11 (0%)
Query 1  ATEAPSSRETG 11
        ATEAPSSRETG
Sbjct 140 ATEAPSSRETG 150
Score = 27.8 bits (58), Expect = 104
Identities = 8/8 (100%), Positives = 8/8 (100%), Gaps = 0/8 (0%)
Query 10 TGAENPEK 17
        TGAENPEK
Sbjct 378 TGAENPEK 385

```

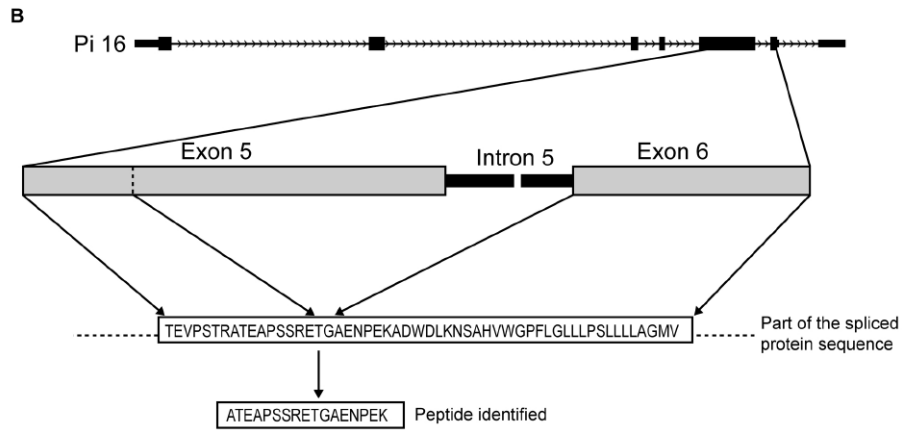


**Figure 2.** A novel variant for peptidase inhibitor 16 was identified by unique peptide ‘ATEAPSSRETGAENPEK’. Figure 2a shows the alignment of this peptide to known pi16 protein sequence by NCBI blastp. The alignment pattern suggests a deletion of 230 amino acids (151-380) in the known protein sequence. Figure 2b shows the schematic representation of alternative splicing in exon 5 of pi16 where the corresponding sequence of the exon was spliced out along with intron 5 in the novel variant.

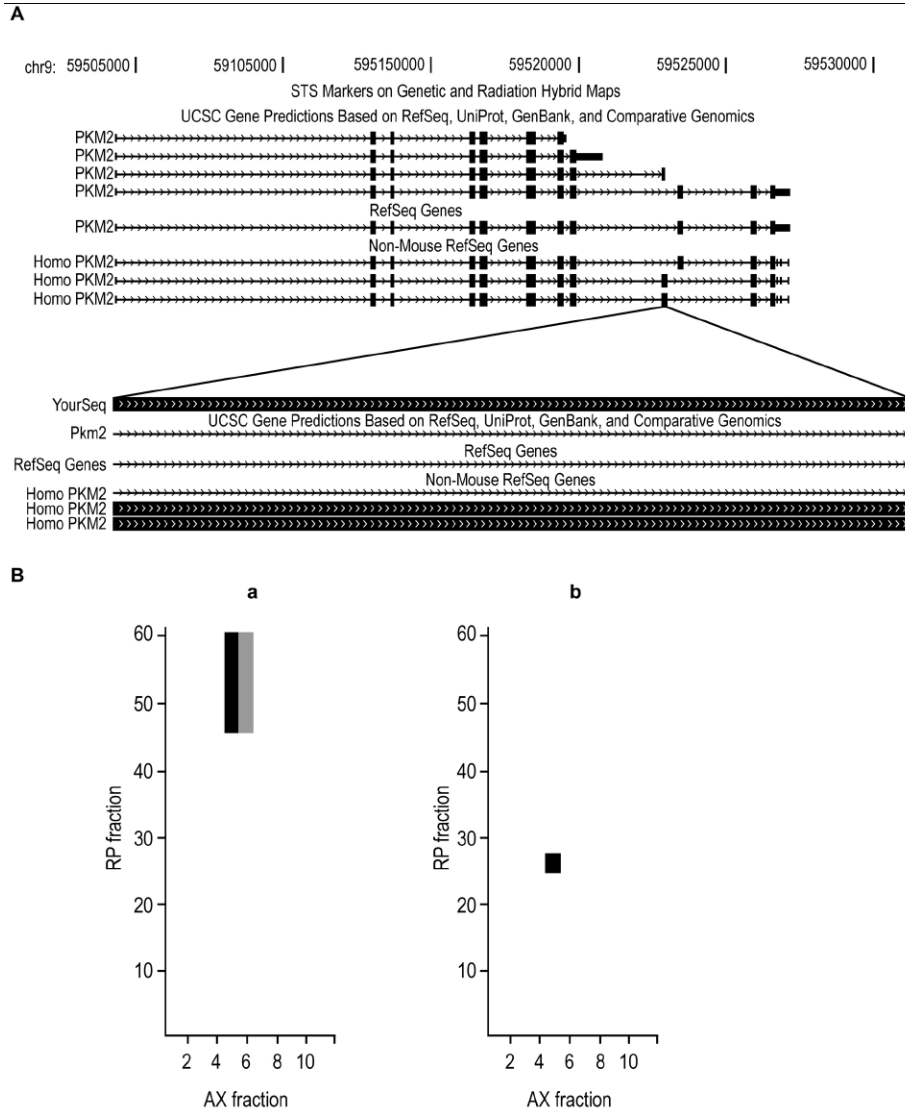


**Figure 3.**  
**3a.** Shown in the upper panel of the figure is the genomic structure of the mouse muscle pyruvate kinase gene as shown on the UCSC Genome Browser. Below is an expanded view of the 42 bp region on chromosome 9 from 59,522,962 to 59,523,003, the genomic mapping of mouse peptide CLAAALIVLTESGR obtained using UCSC Blast program. Mouse splice variant ‘M9C5102\_28\_s74\_e1844\_1\_rf0\_c1\_n0 |’ was identified with 25 distinct peptides. This protein is a splice variant of pyruvate kinase. The 14 amino acids peptide CLAAALIVLTESGR aligns to the coding sequences of human muscle pyruvate kinase, but not to the annotated coding region of mouse muscle pyruvate kinase gene (*pkm2*). The blocked sequence is the coding sequence.  
**3b.** IPAS mapping of splice isoform variants for the malate dehydrogenase 1 gene. Intact proteins were subjected to anion exchange (AX) and reverse phase (RP) chromatography fractionation. Spectral counts for matching peptides derived from this gene are plotted as a function of AX and RP fractionation. The color of each cell indicates the number of matching spectra. Black = high, Grey = low, White = 0. Panel A shows the distribution of spectra matching only the major annotated protein (ENSMUSG0000020321). Panel B shows the distribution of spectra matching only the novel splice isoform

(M11C1527\_1\_s647\_e782\_1\_rf0\_c1\_n0), whose mobility suggests similar charge with much less hydrophobicity.

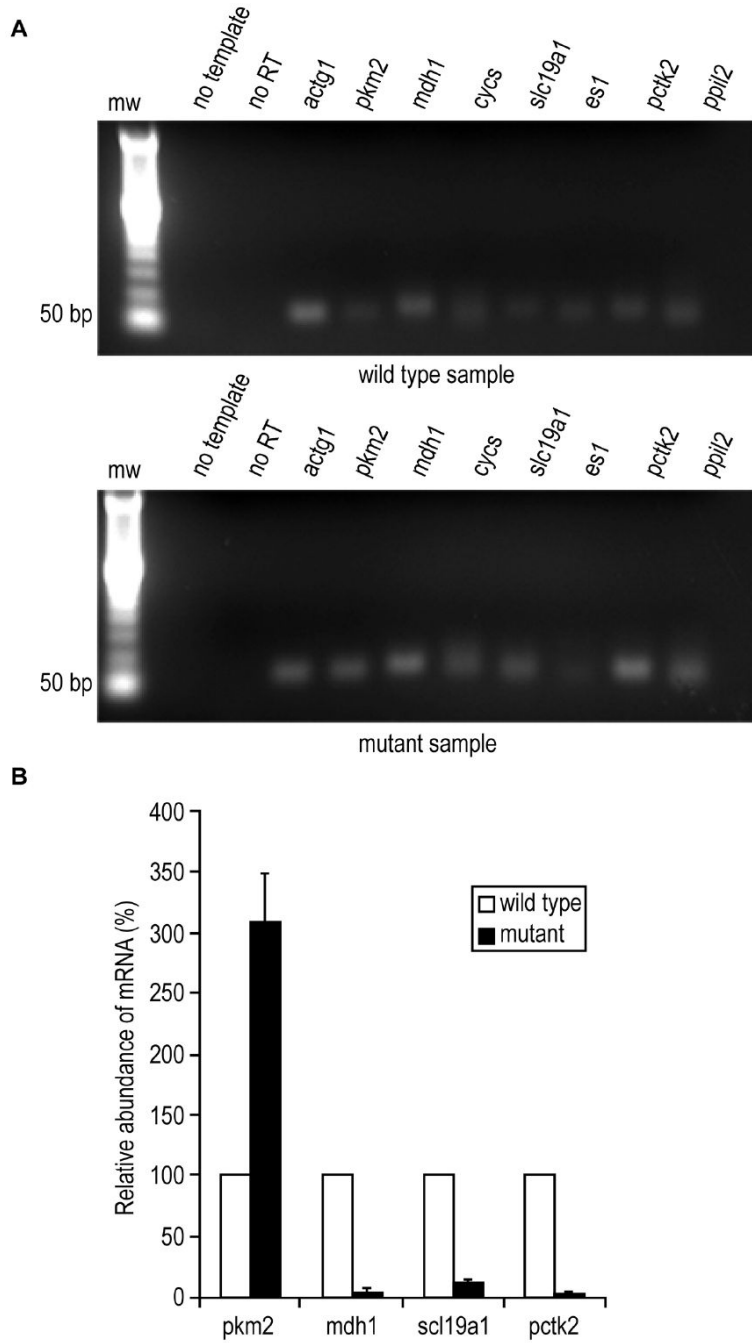


**Figure 4.**

**a)** Electrophoresis gel images showing the RT-PCR amplifications. The original picture was cropped using Adobe Photoshop. RT-PCR analyses of novel variants of gamma actin (*actg1*), pyruvate kinase (*pkm2*), malate dehydrogenase 1 (*mdh1*), cytochrome c somatic (*cycs*), solute carrier family 19 member 1 (*slc19a1*), esterase 1 (*es1*), PCTAIRE-motif protein kinase 2 (*pck2*), and peptidylprolyl isomerase-like 2 (*ppil2*) in pancreas tissue lysates from wild type and mutant mice with pancreatic ductal adenocarcinoma. Gamma actin was used as the internal control. Lane 1 shows molecular weight markers. Lanes 2 and 3 are negative controls. Lane 2 is a reaction with all reagents but with no sample template, and lane 3 has all reagents with actin primers but with no reverse transcriptase. All other lanes are labeled. **b)** Quantification

of mRNA using Real-Time PCR. mRNA levels of the four novel variants were measured in triplicate by real-time quantitative RT-PCR in pancreas tissue lysates of wild type and mutant mice using a SyberGreen PCR assay. The values in the mutant sample are shown relative to the level of expression in the wild type. The bars indicate the mean and standard deviation of the relative expression level in the mutant.

**Table 1**  
Summary of total number of protein and peptide identifications from X!Tandem searches and post search analysis

	TPP analysis <sup>d</sup>	MPP1 analysis <sup>d</sup>	Found in both MPP1 and TPP analyses <sup>a</sup>	Found in either MPP1 or TPP analyses <sup>a</sup>	Non redundant Union <sup>c</sup>
Distinct peptides	8350	7892	6828	9416	9416
Distinct proteins	1150 (16 <sup>b</sup> )	1063 (12 <sup>b</sup> )	873 (3 <sup>b</sup> )	1340 (25 <sup>b</sup> )	1278 (25 <sup>b</sup> )
Alternative splice variant proteins detected	367	352	256	463	420

<sup>a</sup>) Threshold values applied were ProteinProphet probability value > 0.9 and X!Tandem expect value < 0.001.

<sup>b</sup>) The number in parentheses shows the false positive identifications that are from the reverse sequences.

<sup>c</sup>) To remove redundant proteins from the union of TPP and first phase MPP1 analyses, a second round of MPP1 was run on peptides found in both methods.

**Table 2** Quantitative data based on isotopic ratios for levels in plasma for 28 novel alternative splice variant proteins from tumor-bearing mice relative to controls

Identifier	Description	Average expression ratio of the unique peptides (mutant / normal)	Standard error of mean	Multiple spectra for the unique peptides (yes/no)	values of 95% confidence interval (CI)
M8C8688_3_s53_e428_1_rf2_c1_n0	hemopexin variant	6.53	1.19	yes	4.54 - 9.38
M1C9441_5_s110_e3896_1_rf0_c1_n0	complement component factor H variant	3.29	1.09	yes	2.79 - 3.87
M1C9704_2_s2_e1295_1_rf1_c1_n0	proteoglycan 4 variant	5.04	1.32	yes	2.68 - 9.48
M5C6352_7_s782_e884_1_rf1_c1_n0	vitamin d binding protein variant	3.44	1.21	yes	2.27 - 5.20
M11C1527_1_s647_e782_1_rf0_c1_n0	malate dehydrogenase 1, NAD variant	4.17	1.56	yes	1.52 - 11.40
M9C5102_28_s74_e1844_1_rf0_c1_n0	pyruvate kinase variant	2.19	1.19	yes	1.36 - 3.52
ENSMUSG00000073842 ENSMUST000_00079697 ENSMUSP00000078636_s2_e542_1_rf0_c1_n0	Major urinary protein 1 (member of the major urinary protein (Mup) gene family).	1.78	1.05	yes	1.61 - 1.97
M16C2153_1_s11_e218_1_rf1_c1_n0	alpha-2-HS-glycoprotein variant	1.93	1.27	yes	1.00 - 3.72
M4C3970_1_s2_e392_1_rf0_c1_n0	member of the major urinary protein (Mup) gene family	1.01	1.01	yes	0.98 - 1.03
M5C4343_1_s404_e584_1_rf0_c1_n0	glyceraldehyde-3-phosphate dehydrogenase variant	1.02	1.03	yes	0.96 - 1.09
M5C6352_5_s104_e1163_1_rf2_c1_n0	vitamin d binding protein variant	2.1	1.44	yes	0.76 - 5.75
M9C7735_1_s299_e431_1_rf2_c1_n0	PCTAIRE-motif protein kinase 2, isoform CRA_b variant	0.78	1.41	yes	0.60 - 2.75
M8C3753_1_s122_e296_1_rf1_c1_n0	vitamin D-binding protein variant	0.97	1.22	yes	0.51 - 1.84
M6C861_14_s2_e158_1_rf1_c1_n0	capping protein (actin filament) muscle Z-line variant	0.57	1.77	yes	0.15 - 2.10
M13C7050_1_s167_e287_1_rf1_c1_n0	tubulin cofactor a variant	1.32	1.33	yes	--
M7C9387_3_s2_e728_1_rf0_c1_n0	hemopexin variant	1.01	3.09	yes	--
ENSMUSG00000058952 ENSMUST000_00098620 ENSMUSP00000096220_s2_e1805_1_rf0_c1_n0	complement factor i variant	6.67	--	no	--
M7C9387_17_s194_e1220_1_rf0_c1_n0	hemopexin variant	5.26	--	no	--
M1C9426_3_s26_e914_1_rf1_c1_n0	complement component factor H variant	5.26	--	no	--
M18C3726_1_s2_e347_1_rf0_c1_n0	high mobility group protein B2 variant	3.45	--	no	--
M14C7677_1_s356_e431_1_rf1_c1_n0	NULL	3.33	--	no	--
M10C3394_4_s2_e233_1_rf2_c1_n0	Minichromosome maintenance complex component 9 variant	2.7	--	no	--
M1C7134_1_s314_e689_1_rf2_c1_n0	peroxiredoxin 2 variant	1.39	--	no	--
M1C5543_4_s254_e473_1_rf1_c1_n0	solute carrier family 19 (sodium/hydrogen) variant	1.3	--	no	--
M7C9387_1_s92_e434_1_rf1_c1_n0	hemopexin variant	1.1	--	no	--
M1C10834_9_s770_e824_1_rf2_c1_n0	NULL	0.95	--	no	--
M5C5274_1_s2_e95_1_rf0_c1_n0	NULL	0.66	--	no	--
M5C6460_1_s86_e1988_1_rf0_c1_n0	alpha fetoprotein	0.65	--	no	--